

A Computational Study of Lithium Dialkylamide Mixed Aggregates with Lithium Chloride

Lawrence M. Pratt

Department of Chemistry, Fisk University, Nashville TN 37209, USA

Received October 25, 2004; E-mail: lpratt@fisk.edu

Lithium dialkylamides form several mixed aggregates with lithium chloride in ethereal solvents. The relative amounts of mixed dimer, trimer, and tetramer are dependent on the steric strain of the lithium dialkylamide homodimer and on solvent effects. Microsolvation with coordinating THF ligands generated results in qualitative agreement with available experimental data.

Lithium mixed aggregates are complexes between two different lithium compounds that may have chemical properties different from those of either component. The formation of mixed aggregates has been observed for a number of lithium systems, most often in ethereal solvents. Mixed aggregates may be formed in several ways. Lithium salts, such as lithium halides or lithium perchlorate, may be intentionally added to the reaction. Enolization reactions are sometimes performed in the presence of chlorotrimethylsilane to trap the enolate as it forms, and the lithium chloride byproduct can also form mixed aggregates with the lithium dialkylamide.[1] A slight excess of butyllithium is often used when preparing lithium dialkylamides from secondary amines, particularly hindered amines, such as tetramethylpiperidine; the result is a lithium dialkylamide–butyllithium mixed aggregate.[2,3] The exposure of alkyllithiums to small amounts of air results in the formation of lithium oxides, and these can form mixed aggregates with the remaining alkyllithium.[4–7] Lithium enolates are prepared from deprotonation of carbonyl compounds with lithium dialkylamides, and the newly formed enolate can form mixed aggregates with the remaining lithium dialkylamide.[8,9]

The changes in the chemical properties may be minor, with the reactivity of the mixed aggregate differing only slightly from that of the parent organolithium compound, or the mixed aggregate may cause major changes in the chemical reactivity. The formation of mixed aggregates is often discovered by empirical observation of how changes in the reaction conditions change the course of reactions. For example, the use of highly purified lithium reagents may yield a different product distribution than that obtained from reagents that have been exposed to small amounts of air, or from alkyllithium compounds that contain residual lithium halides. Many organic reactions are performed in the presence of lithium salts or other lithium compounds because they generate higher yields or purer products, although the mode of action remains unknown.

Lithium dialkylamide–lithium chloride mixed aggregates were discovered as a result of trapping newly formed enolates with chlorotrimethylsilane when enolization was performed with lithium *t*-octyl-*t*-butylamide.[1] The enolization stereoselectivity was found to vary with the amount of enolate that was formed and, thus, the amount of lithium chloride that was produced from the chlorotrimethylsilane. Collum and co-workers showed that several different lithium dialkylamide mixed aggregates were formed with lithium halides and lithium enolates, and that the amount of lithium halide present in the reaction mixture could dramatically influence the stereochemistry of 3-pentanone enolization.[8,9] Although the structures of the mixed aggregates were determined, the mechanism for the stereoselective enolization remains unknown. A major limitation of lithium NMR, used in those studies, is that the spectra must be acquired at low temperature, ca. −100 °C, to avoid lithium exchange; the previously published NMR study was performed at −115 °C (158 K). Enolization reactions are typically performed at −70 to −80 °C (203–193 K), and sometimes at higher temperatures, and the distribution of mixed aggregates may be temperature dependent. In this paper we used computational methods to investigate the effects of temperature, coordinating solvent ligands, and lithium dialkylamide structure on lithium dialkylamide mixed aggregate formation with lithium chloride.

Computational Methods

All geometry optimizations and frequency calculations were performed using *Gaussian 98* or *Gaussian 03*.[10] The solvation was modeled by microsolvation with explicit dimethyl ether or THF ligands on the lithium atoms. Dimethyl ether is often used to approximate the effects of coordinated THF ligands because of the lower computational cost. Although the use of continuum solvent models in combination with microsolvation sometimes generates slightly better energies than microsolvation alone, the continuum solvent models have proven to be inconsistent with lithium compounds,[11,12] and were not used in this study. The free energies of each species were obtained by adding a thermal correction to the free energy, obtained from the frequency calculations, to the calculated internal energies.

All frequency calculations in the present work were carried out for temperatures of 158, 200, and 298 K. The standard-state molar free energy of a solute in the liquid phase at these temperatures is given by $G^{\circ}_{T}(l) = G^{\circ}_{T}(gas) + \Delta G^{\circ}_{S}$ (T = 158, 200, or 298 K), where l denotes a solute in the liquid

Published on the web May 6, 2005; DOI 10.1246/bcsj.78.890

phase and ΔG°_{S} is the standard-state free energy of solvation. The microsolvation model assumes that ΔG°_{S} is adequately represented by the coordinated ethereal ligands, so that $G^{\circ}_{T}(l) \approx G^{\circ}_{T}(g)$ of the "supermolecule" composed of the organolithium compound plus its coordinated ethereal ligands. Furthermore, $G^{\circ}_{T}(g) = E_{en} + E^{vib}{}_{0} + G^{trans,o}{}_{T} + G^{rot}{}_{T} + G^{vib}{}_{T} + RT$, where R is the gas constant. The individual terms were calculated as follows:

E_{en}, the electronic energy plus nuclear repulsion, by the B3LYP hybrid density functional method[13,14] with the 6-31+G(d) basis set;[15,16]

$E^{vib}{}_{0}$, the $y =$ unscaled zero point energy, by B3LYP calculations with the MIDI![17] basis set;

$G^{trans,o}{}_{T}$, the standard-state thermal translational energy for a standard state of 1 mole per liter (not 1 atm) from the masses;

$G^{rot}{}_{T}$, the thermal rotational free energy, from the B3LYP/MIDI! geometries;

$G^{vib}{}_{T}$, the thermal vibrational free energy, from the unscaled B3LYP/MIDI! vibrational frequencies;

ΔG°_{S}, from B3LYP/6-31+G(d) microsolvated calculations, with a gas phase standard state, as specified above, and a liquid-phase standard state of one mole per liter.

The formulas given above are correct for solutes, and will be applied to $(RLi)_n$ (l) and $(RLi)_n \cdot mE$(liq), where R is an alkyl group, and E is an ether molecule. However, for E(liq), since E is the solvent we must use a standard state of the pure liquid. This requires an extra term:[18] $G^{\circ}_{S}(\text{solvent}) = G^{\circ}_{S}(l) + RT \ln M^{\circ}_{liq}/M^{\circ}_{solvent}$, where M°_{liq} is the standard state molarity of liquid solutes (taken as 1 molar in this work), and $M^{\circ}_{solvent}$ is the molarity of the pure THF solvent, which was calculated in each case from its tabulated density at 158, 200, or 298 K. This term is numerically equal to −1.0273 kcal/mol per THF at 200 K, and −1.4884 kcal/mol at 298 K. Because pure THF is a solid at 158 K, hydrocarbon cosolvents are used for NMR work at this temperature. In order to estimate the $RT \ln M^{\circ}_{liq}/M^{\circ}_{solvent}$ term for THF at 158 K, the density of pure THF was extrapolated to 158 K, and the resulting term was estimated to be −0.8207 kcal/mol per THF at 158 K.

Results and Discussion

The lithium dialkylamides chosen to study were lithium dimethylamide (LiDMA), lithium diisopropylamide (LDA), lithium tetramethylpiperidide (LiTMP), and lithium hexamethyldisilazide (LiHMDS). The 6-31+G(d) basis set was chosen to give an acceptable accuracy at a reasonable computational cost. A recent computational study on lithium enolate mixed aggregates showed that the difference for the calculated aggregation energies between the 6-31+G(d) and 6-311+G(d) basis sets is about 1–3 kcal/mol; most of that difference can likely be attributed to the absence of diffuse functions in the smaller basis set.[19] The 6-31+G(d) basis set was used in the study of several other organolithium compounds, and generally gave results in reasonable agreement with experimental or higher level computational data.[20–22] In order to assess the formation of mixed aggregates in the absence of solvent effects, gas-phase energies were calculated for the formation of mixed dimers, trimers, and tetramers, as shown in Scheme 1. The free energies of mixed dimer, trimer, and tetramer formation are given in Tables 1–5, along with the calculated equilibrium constants; and the optimized geometries are shown in Figs. 1–4. The aggregation energies were obtained form the $LiNR_2$ and LiCl dimers. Although LiTMP has been shown to be a trimer–tetramer mixture in pentane,[23] and those struc-

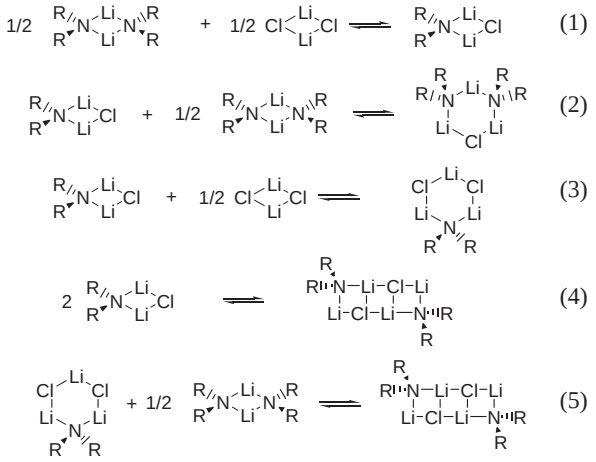

Scheme 1. Gas-phase mixed aggregate formation.

Table 1. Free Energy and Equilibrium Constants of Gas Phase Mixed Dimer Formation (Scheme 1, Reaction 1)

$LiNR_2$	T/K	ΔG°_{f} mixed dimer /kcal mol^{-1}	K
LiDMA	158	−1.38	81.1
LiDMA	200	−1.43	36.6
LiDMA	298	−1.54	13.6
LDA	158	−1.77	278
LDA	200	−1.87	112
LDA	298	−2.12	36.1
LiTMP	158	−4.71	3.29×10^{6}
LiTMP	200	−4.84	1.97×10^{5}
LiTMP	298	−5.15	5.95×10^{3}
LiHMDS	158	−2.58	3.70×10^{3}
LiHMDS	200	−2.82	1.20×10^{3}
LiHMDS	298	−3.39	3.06×10^{2}

Table 2. Free Energy and Equilibrium Constants of Gas Phase $(LiNR_2)_2LiCl$ Mixed Trimer Formation (Scheme 1, Reaction 2)

$LiNR_2$	T/K	ΔG°_{f} mixed trimer /kcal mol^{-1}	K
LiDMA	158	−14.84	3.42×10^{20}
LiDMA	200	−14.13	2.76×10^{15}
LiDMA	298	−12.54	1.58×10^{9}
LDA	158	−13.18	1.71×10^{18}
LDA	200	−12.26	2.47×10^{13}
LDA	298	−10.17	2.87×10^{7}
LiTMP	158	−11.44	6.59×10^{15}
LiTMP	200	−10.29	1.76×10^{11}
LiTMP	298	−7.66	4.14×10^{5}
LiHMDS	158	−6.56	1.20×10^{9}
LiHMDS	200	−5.48	9.85×10^{5}
LiHMDS	298	−3.03	1.67×10^{2}

Table 3. Free Energy and Equilibrium Constants of Gas Phase $(LiNR_2)(LiCl)_2$ Mixed Trimer Formation (Scheme 1, Reaction 3)

$LiNR_2$	T/K	ΔG°_f mixed trimer /kcal mol^{-1}	K
LiDMA	158	−15.30	1.43×10^{21}
LiDMA	200	−14.66	1.05×10^{16}
LiDMA	298	−13.26	5.30×10^{9}
LDA	158	−15.30	1.44×10^{21}
LDA	200	−14.65	1.01×10^{16}
LDA	298	−13.20	4.84×10^{9}
LiTMP	158	−15.45	2.35×10^{21}
LiTMP	200	−14.85	1.68×10^{16}
LiTMP	298	−13.52	8.24×10^{9}
LiHMDS	158	−14.62	1.67×10^{20}
LiHMDS	200	−14.15	2.87×10^{15}
LiHMDS	298	−13.12	4.20×10^{9}

Table 4. Free Energy and Equilibrium Constants of Gas Phase $(LiNR_2)(LiCl)_2$ Mixed Tetramer Formation (Scheme 1, Reaction 4)

$LiNR_2$	T/K	ΔG°_f mixed trimer /kcal mol^{-1}	K
LiDMA	158	−22.45	3.70×10^{31}
LiDMA	200	−21.45	2.73×10^{23}
LiDMA	298	−18.34	2.83×10^{13}
LDA	158	−20.35	1.40×10^{28}
LDA	200	−18.57	1.93×10^{20}
LDA	298	−14.45	3.96×10^{10}
LiTMP	158	−21.20	2.08×10^{28}
LiTMP	200	−19.60	2.60×10^{21}
LiTMP	298	−15.88	4.44×10^{11}
LiHMDS	158	−19.31	5.17×10^{26}
LiHMDS	200	−17.54	1.47×10^{19}
LiHMDS	298	−13.51	8.15×10^{9}

Table 5. Free Energy and Equilibrium Constants of Gas Phase $(LiNR_2)(LiCl)_2$ Mixed Tetramer Formation from Mixed Trimer and Lithium Dialkylamide Dimer (Scheme 1, Reaction 5)

$LiNR_2$	T/K	ΔG°_f mixed trimer /kcal mol^{-1}	K
LiDMA	158	−8.91	2.09×10^{12}
LiDMA	200	−8.22	9.55×10^{8}
LiDMA	298	−6.63	7.25×10^{4}
LDA	158	−6.82	2.70×10^{9}
LDA	200	−5.79	2.15×10^{6}
LDA	298	−3.37	295
LiTMP	158	−10.46	2.92×10^{14}
LiTMP	200	−9.59	3.05×10^{10}
LiTMP	298	−7.50	3.21×10^{5}
LiHMDS	158	−7.27	1.15×10^{10}
LiHMDS	200	−6.21	6.15×10^{6}
LiHMDS	298	−3.78	594

tures are presumably similar to those in the gas phase, the $LiNR_2$ dimers were used to allow a direct comparison with the structures in ethereal solvents.

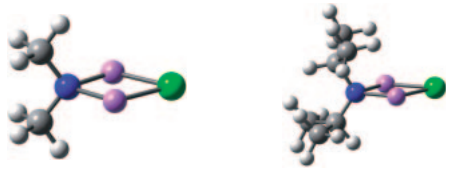

LiDMA (**1a**) LDA (**2a**)

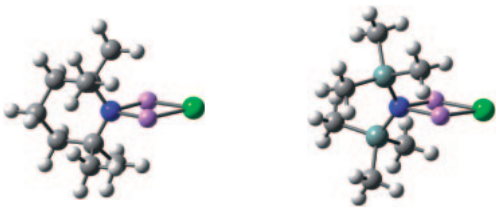

LiTMP (**3a**) LiHMDS (**4a**)

Fig. 1. Optimized geometries of gas phase mixed dimers. Grey: carbon or silicon; white: hydrogen; blue: nitrogen; violet: lithium; green: chlorine.

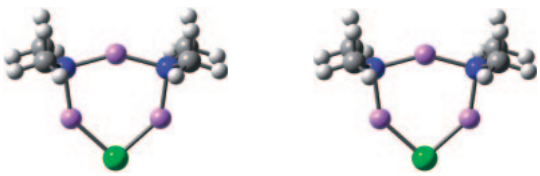

LiDMA (**5a**) LDA (**6a**)

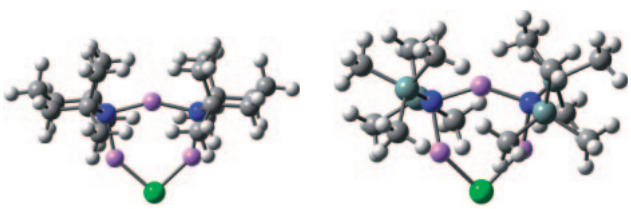

LiTMP (**7a**) LiHMDS (**8a**)

Fig. 2. Optimized geometries of gas phase $(LiNR_2)_2LiCl$ mixed trimer.

The formation of solvated mixed aggregates is shown in Scheme 2, where each aggregate is microsolvated with dimethyl ether or THF. From the calculated energies, it becomes apparent that the use of dimethyl ether as a computationally less-demanding substitute for THF causes large errors in the free energies of formation of the mixed aggregates, as shown in Tables 6–10. Zero, one, or two solvent ligands were used on each lithium atom. For all lithium dialkylamides, except for lithium dimethylamide (LiDMA), only one ether or THF per lithium was permitted by steric effects, and LiDMA was similarly modeled for consistency. A similar solvation scheme was used for the mixed dimers, except that a third solvent ligand was also used for a comparison with previously published experimental work, as described below. In all other molecules, one solvent ligand was used on each lithium, except where steric crowding prevented microsolvation of one lithium atom, as in reaction 7.

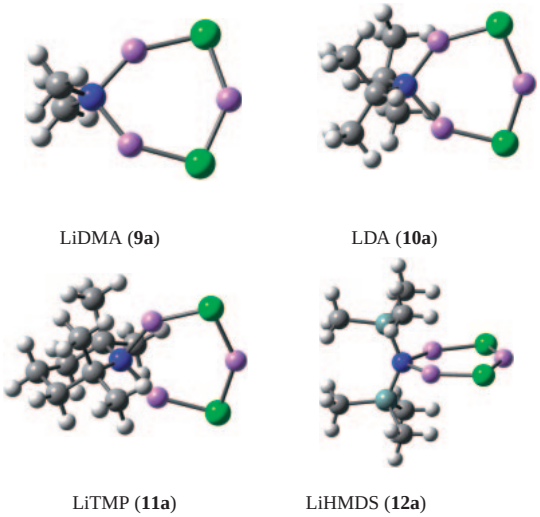

Fig. 3. Optimized geometries of gas phase $(LiNR_2)(LiCl)_2$ mixed trimer.

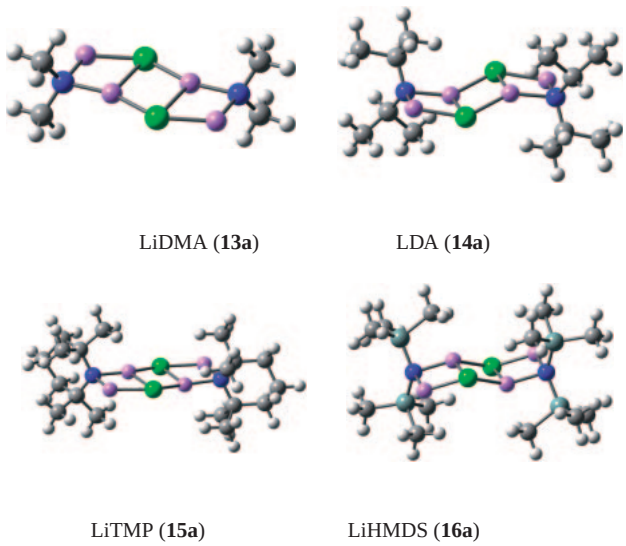

Fig. 4. Optimized geometries of gas phase $(LiNR_2)(LiCl)_2$ mixed tetramer.

The optimized geometries of dimethyl ether and THF solvated mixed dimers are shown in Fig. 5. In both the gas phase and solution, the more sterically hindered LiTMP and LiHMDS showed the greatest tendency to form mixed dimers with lithium chloride. In contrast to LDA, for which the only NMR observable species is the dimer in a THF solution,[24] LiTMP has been observed as a mixture of about 90% dimer and 10% monomer,[25] and LiHMDS is predominantly monomer in THF, in equilibrium with dimer.[26] For consistency, however, the solvated LiHMDS dimer was used to determine the free energies of mixed aggregate formation. Mixed dimer formation (Scheme 2, reaction 6) helps to relieve the steric strain of the bulky alkyl groups across the 4-membered lithium–nitrogen ring. Increasing the steric bulk of the solvent ligands (dimethyl ether to THF) also favored the formation of a mixed dimer. These results are summarized in Table 6.

As in the gas phase calculations, two different solvated

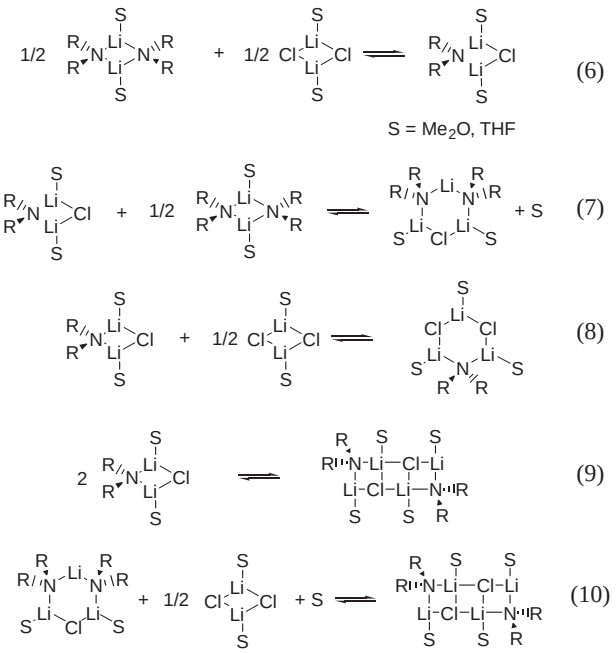

Scheme 2. Solvated mixed aggregate formation.

Table 6. Free Energy and Equilibrium Constants of Solvated Mixed Dimer Formation (Scheme 2, Reaction 6)

$LiNR_2$·Solvent	T/K	ΔG°_f mixed dimer /kcal mol^{-1}	K
LiDMA Me_2O	158	−0.967	21.8
LiDMA Me_2O	200	−0.935	10.5
LiDMA Me_2O	298	−0.778	3.72
LiDMA THF	158	−1.57	146
LiDMA THF	200	−1.68	69.4
LiDMA THF	298	−1.91	25.1
LDA Me_2O	158	−2.81	7.71×10^3
LDA Me_2O	200	−2.59	680
LDA Me_2O	298	−2.03	30.8
LDA THF	158	−3.21	2.74×10^4
LDA THF	200	−3.16	2.85×10^3
LDA THF	298	−3.02	163
LiTMP Me_2O	158	−8.55	6.74×10^{11}
LiTMP Me_2O	200	−8.59	2.44×10^9
LiTMP Me_2O	298	−8.63	2.15×10^6
LiTMP THF	158	−9.28	6.92×10^{12}
LiTMP THF	200	−9.55	2.71×10^{10}
LiTMP THF	298	−10.09	2.52×10^7
LiHMDS Me_2O	158	−3.25	3.19×10^4
LiHMDS Me_2O	200	−2.99	1.84×10^3
LiHMDS Me_2O	298	−2.75	104
LiHMDS THF	158	−6.05	2.36×10^8
LiHMDS THF	200	−6.42	1.04×10^7
LiHMDS THF	298	−7.35	2.46×10^5

mixed trimers could potentially be formed, as shown in reactions 7 and 8. The structures are shown in Figs. 6 and 7, respectively. In the presence of solvating ligands, however, the $(LiNR_2)_2(LiCl)$ mixed trimer is the most energetically favored. The LiDMA mixed trimer has previously been reported as a trisolvate.[19] However, with LDA, LiTMP, and LiHMDS, only

Table 7. Free Energy and Equilibrium Constants of Solvated $(LiNR_2)_2LiCl$ Mixed Trimer Formation (Scheme 2, Reaction 7)

$LiNR_2$·Solvent	T/K	ΔG°_f mixed trimer /kcal mol^{-1}	K
LiDMA Me_2O	158	−3.29	3.57×10^4
LiDMA Me_2O	200	−4.10	3.02×10^4
LiDMA Me_2O	298	−5.87	2.02×10^4
LiDMA THF	158	−0.48	4.65
LiDMA THF	200	−1.52	45.4
LiDMA THF	298	−3.81	626
LDA Me_2O	158	−2.39	1.67×10^3
LDA Me_2O	200	−3.02	2.00×10^3
LDA Me_2O	298	−4.59	2.31×10^3
LDA THF	158	−0.0619	1.22
LDA THF	200	−1.04	13.8
LDA THF	298	−3.19	217
LiTMP Me_2O	158	−6.32	5.46×10^8
LiTMP Me_2O	200	−7.26	8.52×10^7
LiTMP Me_2O	298	−9.31	6.72×10^6
LiTMP THF	158	−1.30	62.8
LiTMP THF	200	−2.01	156
LiTMP THF	298	−3.60	433
LiHMDS Me_2O	158	−1.39	82.8
LiHMDS Me_2O	200	−1.92	124
LiHMDS Me_2O	298	−3.50	371
LiHMDS THF	158	1.80	3.21×10^{-3}
LiHMDS THF	200	0.907	0.10
LiHMDS THF	298	−1.17	7.19

Table 8. Free Energy and Equilibrium Constants of Solvated $(LiNR_2)(LiCl)_2$ Mixed Trimer Formation (Scheme 2, Reaction 8)

$LiNR_2$·Solvent	T/K	ΔG°_f mixed trimer /kcal mol^{-1}	K
LiDMA Me_2O	158	−2.23	1.20×10^3
LiDMA Me_2O	200	−1.33	28.4
LiDMA Me_2O	298	1.13	0.148
LiDMA THF	158	−1.35	74.1
LiDMA THF	200	−0.466	3.23
LiDMA THF	298	1.82	4.66×10^{-2}
LDA Me_2O	158	1.78	3.42×10^{-3}
LDA Me_2O	200	3.09	4.24×10^{-4}
LDA Me_2O	298	6.12	3.26×10^{-5}
LDA THF	158	−0.972	22.1
LDA THF	200	−0.119	1.35
LDA THF	298	2.19	2.49×10^{-2}
LiTMP Me_2O	158	1.74	3.88×10^{-3}
LiTMP Me_2O	200	2.96	5.80×10^{-4}
LiTMP Me_2O	298	5.81	5.44×10^{-5}
LiTMP THF	158	1.21	2.12×10^{-2}
LiTMP THF	200	2.43	2.21×10^{-3}
LiTMP THF	298	5.12	1.76×10^{-4}
LiHMDS Me_2O	158	1.44	1.00×10^{-2}
LiHMDS Me_2O	200	2.68	1.19×10^{-3}
LiHMDS Me_2O	298	5.53	8.73×10^{-5}
LiHMDS THF	158	1.36	1.33×10^{-2}
LiHMDS THF	200	2.43	2.20×10^{-3}
LiHMDS THF	298	4.91	2.52×10^{-4}

Table 9. Free Energy and Equilibrium Constants of Solvated $(LiNR_2)(LiCl)_2$ Mixed Tetramer Formation (Scheme 2, Reaction 9)

$LiNR_2$·Solvent	T/K	ΔG°_f mixed trimer /kcal mol^{-1}	K
LiDMA Me_2O	158	−3.48	6.45×10^4
LiDMA Me_2O	200	−1.52	46.3
LiDMA Me_2O	298	3.12	5.11×10^{-3}
LiDMA THF	158	−1.00	24.4
LiDMA THF	200	1.47	2.48×10^{-2}
LiDMA THF	298	7.34	4.10×10^{-6}
LDA Me_2O	158	1.43	1.04×10^{-2}
LDA Me_2O	200	3.51	1.47×10^{-4}
LDA Me_2O	298	8.40	6.95×10^{-7}
LDA THF	158	1.76	3.64×10^{-3}
LDA THF	200	4.16	2.83×10^{-5}
LDA THF	298	9.53	1.02×10^{-7}
LiTMP Me_2O	158	4.03	2.70×10^{-6}
LiTMP Me_2O	200	6.39	1.03×10^{-7}
LiTMP Me_2O	298	11.72	2.55×10^{-9}
LiTMP THF	158	7.36	6.44×10^{-11}
LiTMP THF	200	10.19	7.39×10^{-12}
LiTMP THF	298	16.43	8.93×10^{-13}
LiHMDS Me_2O	158	4.88	1.79×10^{-7}
LiHMDS Me_2O	200	7.28	1.10×10^{-8}
LiHMDS Me_2O	298	12.80	4.13×10^{-10}
LiHMDS THF	158	7.93	1.06×10^{-11}
LiHMDS THF	200	10.94	1.10×10^{-12}
LiHMDS THF	298	17.89	7.54×10^{-14}

Table 10. Free Energy and Equilibrium Constants of Solvated $(LiNR_2)(LiCl)_2$ Mixed Tetramer Formation from Mixed Trimer and Lithium Chloride Dimer (Scheme 2, Reaction 10)

$LiNR_2$·Solvent	T/K	ΔG°_f mixed trimer /kcal mol^{-1}	K
LiDMA Me_2O	158	4.74	2.80×10^{-7}
LiDMA Me_2O	200	1.64	1.61×10^{-2}
LiDMA Me_2O	298	8.22	9.41×10^{-7}
LiDMA THF	158	7.31	7.80×10^{-11}
LiDMA THF	200	1.30	3.79×10^{-2}
LiDMA THF	298	9.25	1.64×10^{-7}
LDA Me_2O	158	0.559	0.169
LDA Me_2O	200	3.94	4.98×10^{-5}
LDA Me_2O	298	10.95	9.26×10^{-9}
LDA THF	158	5.74	1.15×10^{-8}
LDA THF	200	2.05	5.83×10^{-3}
LDA THF	298	9.70	7.68×10^{-8}
LiTMP Me_2O	158	−1.10	33.8
LiTMP Me_2O	200	5.06	2.95×10^{-6}
LiTMP Me_2O	298	12.39	8.12×10^{-10}
LiTMP THF	158	4.02	7.21×10^{-6}
LiTMP THF	200	2.65	1.28×10^{-3}
LiTMP THF	298	9.93	5.19×10^{-8}
LiHMDS Me_2O	158	−3.52	7.44×10^{-4}
LiHMDS Me_2O	200	6.21	1.64×10^{-7}
LiHMDS Me_2O	298	13.55	1.15×10^{-10}
LiHMDS THF	158	2.48	3.76×10^{-4}
LiHMDS THF	200	3.61	1.13×10^{-4}
LiHMDS THF	298	11.71	2.57×10^{-9}

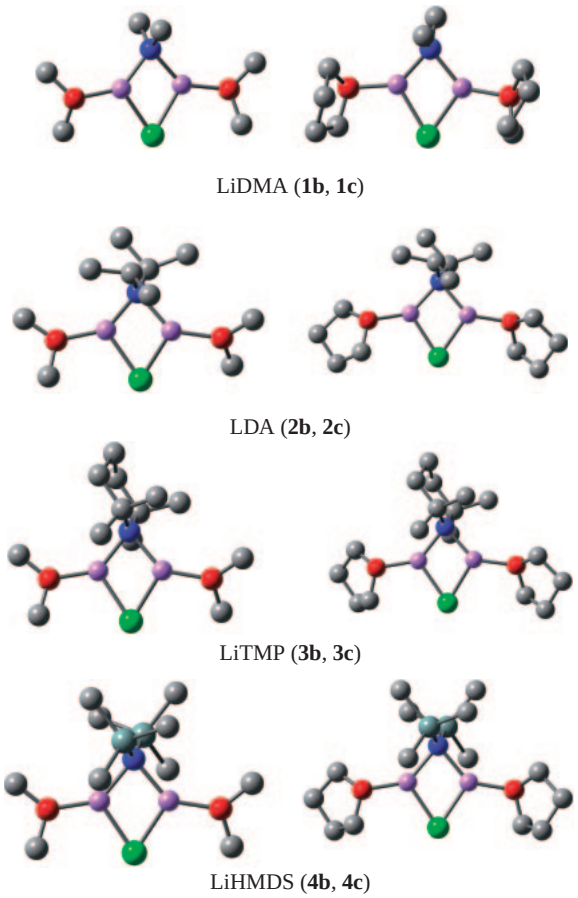

Fig. 5. Optimized geometries of dimethyl ether (**b**) and THF (**c**) solvated mixed dimers. Hydrogen atoms omitted for clarity.

the disolvated form was stable and, for consistency, this species was used in the free-energy calculations.

The data in Table 7 show that the use of dimethyl ether as an approximation for the solvating effects of THF results in significantly more negative free energies of mixed trimer formation, and correspondingly higher calculated equilibrium constants. Even with THF as the solvent, LiDMA was predicted to form significant amounts of mixed trimer, and the tendency to form mixed trimer decreased with increasing the steric bulk in going from LiDMA to LDA to LiHMDS. LiTMP is an exception to this trend, since the calculations showed an unusual tendency to form a mixed trimer, compared to the other lithium dialkylamides. Collum and co-workers proposed a LiTMP–LiCl mixed trimer structure (**7c**) in which the piperidine rings adopted a conformation that minimized the steric strain.[9]

The calculations predicted that LiTMP and LiHMDS will not form the $(LiCl)_2(LiNR_2)$ mixed trimer, and that LiDMA will form the $(LiNR_2)_2(LiCl)$ mixed trimer in preference to $(LiCl)_2(LiNR_2)$. LDA showed a slight energetic preference for the $(LiCl)_2(LiNR_2)$ in THF at 158 K, but favored the $(LiNR_2)_2(LiCl)$ mixed trimer at higher temperatures, as shown from a comparison of the data in Tables 7 and 8.

The optimized geometries of a solvated $(LiNR_2)(LiCl)_2$ mixed tetramer, analogous to those reported with LiTMP and lithium enolates,[9] are shown in Fig. 8. Each of the tetramers

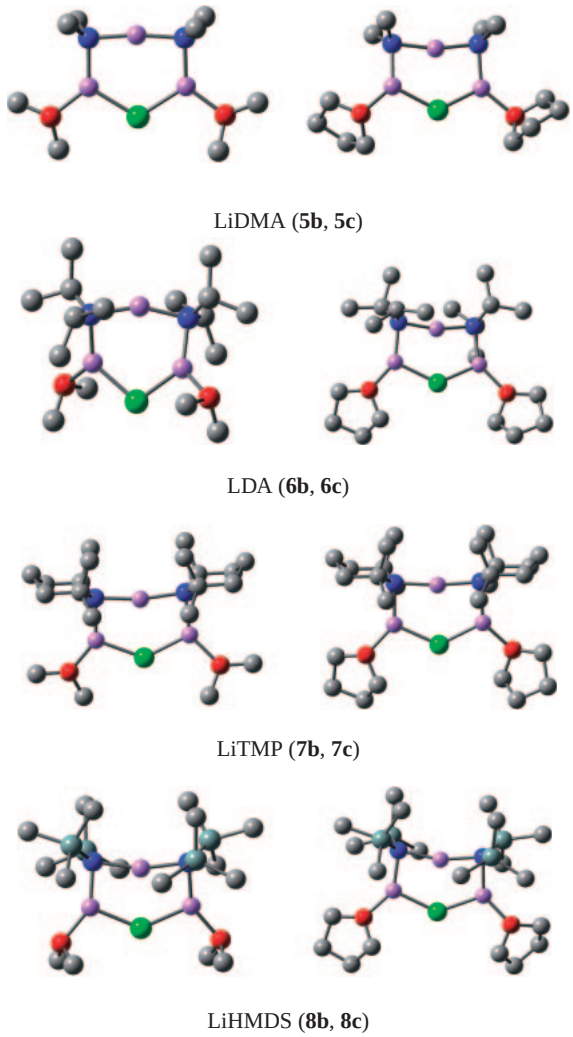

Fig. 6. Optimized geometries of dimethyl ether (**b**) and THF (**c**) solvated $(LiNR_2)_2LiCl$ mixed trimers.

formed a bent ladder structure, similar to the gas-phase structures.

The free energies of solvated tetramer formation from the dimer are given in Table 9, and from the most stable $(LiNR_2)_2LiCl$ mixed trimer and lithium chloride dimer in Table 10. Significant amounts of tetramer are predicted to form from the dimer only with LiDMA at low temperatures. When dimethyl ether was used in place of THF for microsolvation, LDA and LiTMP mixed trimers (**6b** and **7b**) were predicted to form some mixed tetramer with excess LiCl at low temperatures. LDA, LiTMP, and LiHMDS were all predicted not to form significant amounts of tetramer with THF microsolvation.

The computational results of THF solvated LiTMP mixed aggregate formation can be compared to the previously published NMR results reported at 158 K.[9] In a 0.1 M solution of LiTMP with 0.3 equivalents of LiCl, both the mixed trimer (**7c**) and free LiTMP were observed. The mixed trimer was actually observed in two different conformations, presumed to be the most stable conformation shown in Fig. 5, and a minor conformation from a piperidine ring flip. At 0.6 equivalents of LiCl, both the mixed trimer (in both conformations) and

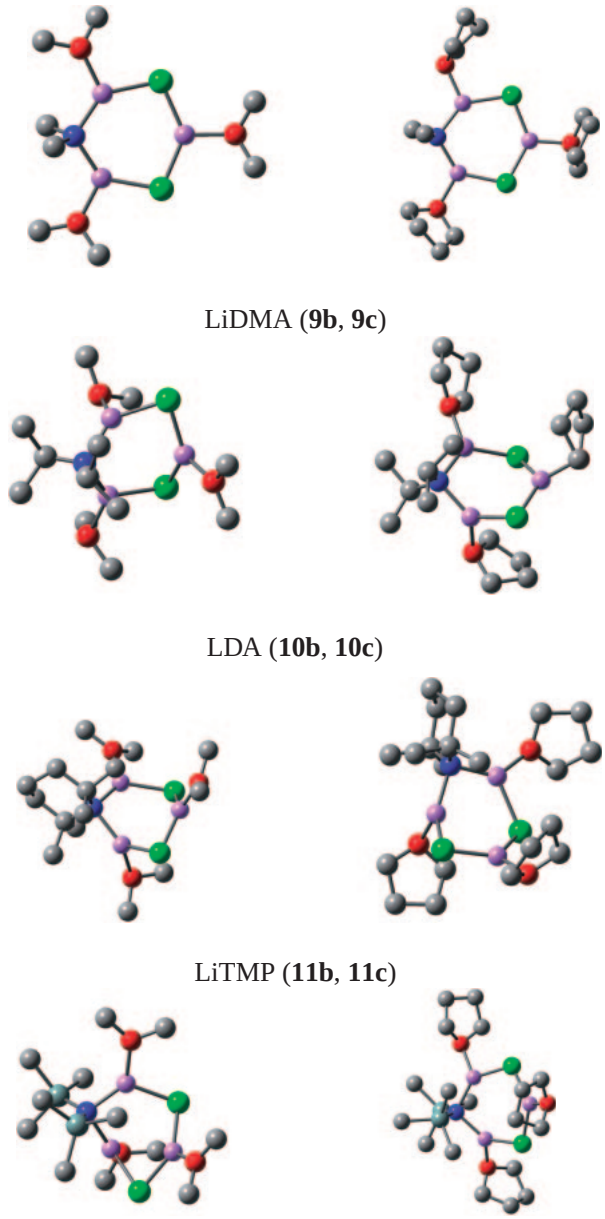

Fig. 7. Optimized geometries of dimethyl ether (**b**) and THF (**c**) solvated $(LiNR_2)(LiCl)_2$ mixed trimers.

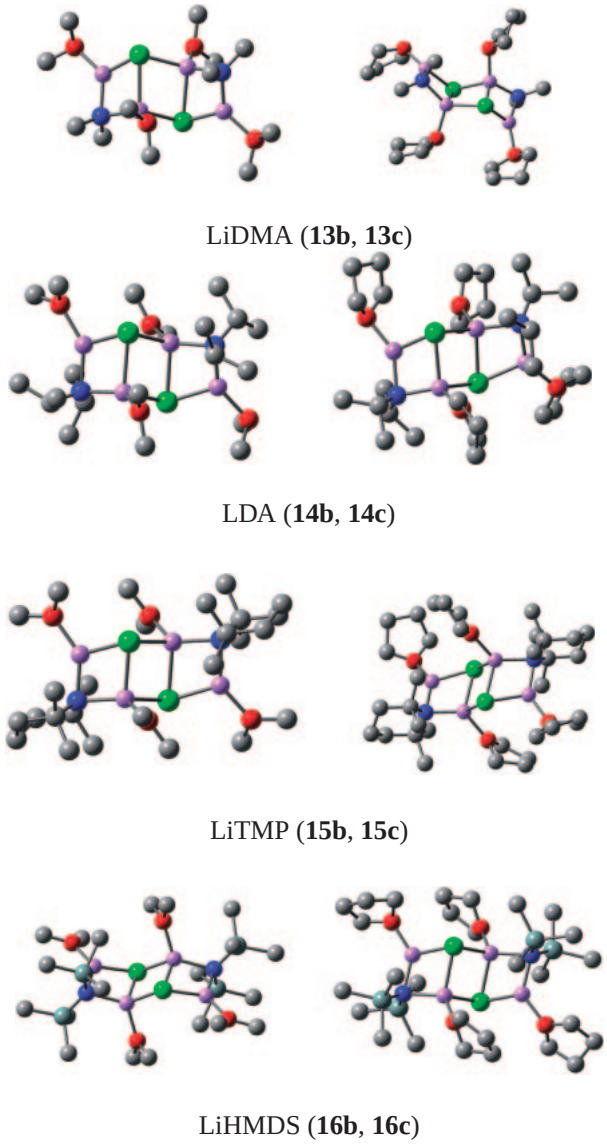

Fig. 8. Optimized geometries of dimethyl ether (**b**) and THF (**c**) solvated $(LiNR_2)_2(LiCl)_2$ mixed tetramers.

the mixed dimer (**3c**) were reported, with no free LiTMP. When 1.2 equivalents of LiCl were added, the major species present was the mixed dimer, along with free lithium chloride and a small amount of mixed trimer.

The calculated free-energy of LiTMP dimerization predicts it to form mixed aggregates with LiCl to the exclusion of free LiTMP, which is consistent with the published data. The free energy calculations at 158 K also predict an equilibrium constant of 62.8 for the reaction illustrated in reaction 7, with both the mixed dimer and the mixed trimer present with 0.6 equivalents of LiCl. This prediction is in remarkably good agreement with the experimental work, and indicates that the calculation was accurate to within about ±2 kcal/mol. It is also noteworthy that the use of dimethyl ether in place of THF predicted the same equilibrium constant to be 5.46×10^8. Thus, the computationally less demanding dimethyl ether ligand is not a satisfactory substitute for THF in predicting the aggregation states of lithium dialkylamides.

The calculated structures of the mixed aggregates were generally in qualitative agreement with those reported for LDA and LiTMP using MNDO semiempirical calculations.[27] In both Romesberg and Collum's semiempirical, and our DFT calculations, the trimers formed a six-membered ring rather than the ladder structures that were reported by X-ray crystallography on related systems.[28,29] The latter study also reported THF trisolvated LiTMP–LiBr mixed dimers. Additional geometry optimizations were performed on the analogous $LiNR_2$–LiCl THF trisolvated mixed dimers, formed from the disolvated mixed dimers, according to Eq. 11. The results are presented in Table 11. The corresponding optimized geometries are shown in Fig. 9. Unlike the solid-state structures of LiBr mixed

Table 11. Calculated Free Energies of the Third Solvation of $LiNR_2$–LiCl Mixed Dimers (Eq. 11)

$LiNR_2$	T/K	ΔG° 3rd solvatio /kcal mol^{-1}	K
LiDMA	158	−2.71	5.57×10^{3}
LiDMA	200	−0.805	7.59
LiDMA	298	3.49	2.76×10^{-3}
LDA	158	−0.736	10.4
LDA	200	1.03	7.53×10^{-2}
LDA	298	4.98	2.24×10^{-4}
LiTMP	158	4.39	8.40×10^{-7}
LiTMP	200	6.39	1.03×10^{-7}
LiTMP	298	10.8	1.10×10^{-8}
LiHMDS	158	0.552	0.173
LiHMDS	200	2.42	2.27×10^{-3}
LiHMDS	298	6.68	1.26×10^{-5}

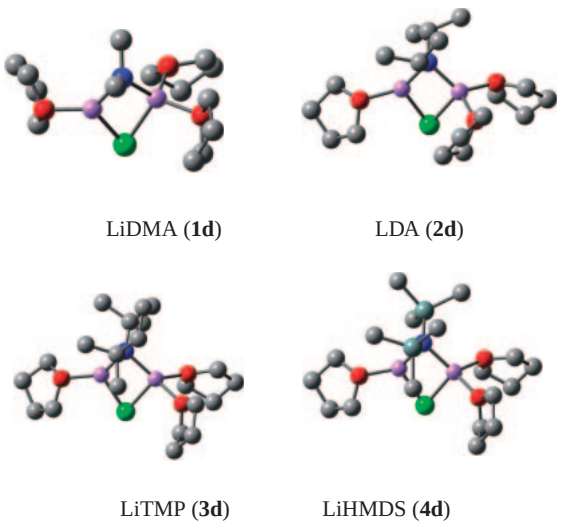

LiDMA (**1d**) LDA (**2d**)

LiTMP (**3d**) LiHMDS (**4d**)

Fig. 9. Optimized geometries of $LiNR_2$–LiCl THF trisolvated mixed dimers.

dimers, LiTMP and LiHMDS do not appear to form the THF trisolvated structures to a large extent, and LiDMA and LDA do so only at low temperatures. The difference is likely to be due, at least in part, to the longer Li–X bond lengths in the LiBr mixed aggregates compared to the LiCl mixed aggregates.

$$LiNR_2\text{–}LiCl\cdot 2THF + THF \rightarrow LiNR_2\text{–}LiCl\cdot 3THF \qquad (11)$$

Conclusion

LiDMA, LDA, LiTMP, and LiHMDS all form mixed aggregates in the gas phase and in a THF solution with lithium chloride. Mixed aggregate formation is temperature dependent, and the distribution of mixed aggregates that were reported from NMR experiments will not necessarily be the same as the mixed aggregate distribution at higher temperatures commonly used in synthetic reactions. In the gas phase, tetramers are the predominant species, with increased steric strain disfavoring tetramer formation. The calculations predicted dimer and trimer formation of LDA, LiTMP, and LiHMDS in THF solution, with only LiDMA forming the tetramer at low temperatures. Microsolvation with dimethyl ether incorrectly predicted mixed aggregate formation of LiTMP with lithium chloride, but microsolvation with THF ligands gave results in good agreement with the published experimental data.

This work was supported in part by the NIH-MBRS grant #S06-GM62813-01 and NSF grant #CHE-0139076.

Supporting Information

Tables of optimized geometries and energies of compounds **1**–**16**. This material is available free of charge on the web at http://www.csj.jp/journals/bcsj/.

References

1 E. J. Corey and A. W. Gross, *Tetrahedron Lett.*, **25**, 495 (1984).

2 L. M. Pratt, A. Newman, J. St. Cyr, H. Johnson, B. Miles, A. Lattier, E. Austin, S. Henderson, B. Hershey, M. Lin, Y. Balamraju, L. Sammonds, J. Cheramie, J. Karnes, E. Hymel, B. Woodford, and C. Carter, *J. Org. Chem.*, **68**, 6387 (2003).

3 Y. Balamraju, C. D. Sharp, W. Gammill, N. Manuel, and L. M. Pratt, *Tetrahedron*, **54**, 7357 (1998).

4 L. M. Seitz and T. L. Brown, *J. Am. Chem. Soc.*, **88**, 2174 (1966).

5 J. F. McGarrity and C. A. Ogle, *J. Am. Chem. Soc.*, **107**, 1805 (1985).

6 T. Kremer, S. Harder, M. Junge, and P. v. R. Schleyer, *Organometallics*, **15**, 585 (1996).

7 J. F. McGarrity, C. A. Ogle, Z. Brich, and H.-R. Loosli, *J. Am. Chem. Soc.*, **107**, 1810 (1985).

8 P. L. Hall, J. H. Gilchrist, and D. B. Collum, *J. Am. Chem. Soc.*, **113**, 9571 (1991).

9 P. L. Hall, J. H. Gilchrist, A. T. Harrison, D. B. Fuller, and D. B. Collum, *J. Am. Chem. Soc.*, **113**, 9575 (1991).

10 M. J. Frisch, G. W. Trucks, H. B. Schlegel, G. E. Scuseria, M. A. Robb, J. R. Cheeseman, J. A. Montgomery, Jr., T. Vreven, K. N. Kudin, J. C. Burant, J. M. Millam, S. S. Iyengar, J. Tomasi, V. Barone. B. Mennucci, M. Cossi, G. Scalmani, N. Rega, G. A. Petersson, H. Nakatsuji, M. Hada, M. Ehara, K. Toyota, R. Fukuda, J. Hasegawa, M. Ishida, T. Nakajima, Y. Honda, O. Kitao, H. Nakai, M. Klene, X. Li, J. E. Knox, H. P. Hratchian, J. B. Cross, C. Adamo, J. Jaramillo, R. Gomperts, R. E. Stratmann, O. Yazyev, A. J. Austin, R. Cammi, C. Pomelli, J. W. Ochterski, P. Y. Ayala, K. Morokuma, G. A. Voth, P. Salvador, J. J. Dannenberg, V. G. Zakrzewski, S. Dapprich, A. D. Daniels, M. C. Strain, O. Farkas, D. K. Malick, A. D. Rabuck, K. Raghavachari, J. B. Foresman, J. V. Ortiz, Q. Cui, A. G. Baboul, S. Clifford, J. Cioslowski, B. B. Stefanov, G. Liu, A. Liashenko, P. Piskortz, I. Komaromi, R. L. Martin, D. J. Fox, T. Keith, M. A. Al-Laham, C. Y. Peng, A. Nanayakkara, M. Challacombe, P. M. W. Gill, B. Johnson, W. Chem, M. W. Wong, C. Gonzalez, and J. A. Pople, "Gaussian 03, Revision A.1," Gaussian, Inc., Pittsburgh, PA (2003).

11 L. M. Pratt, B. Ramachandran, J. D. Xidos, C. J. Cramer, and D. G. Truhlar, *J. Org. Chem.*, **67**, 7607 (2002).

12 L. M. Pratt, D. G. Truhlar, C. J. Cramer, S. R. Kass, and J. D. Thompson, work in progress.

13 A. D. Becke, *J. Chem. Phys.*, **98**, 5648 (1993).

14 P. J. Stephens, F. J. Devlin, G. C. Chabalowski, and M. J. Frisch, *J. Phys. Chem.*, **98**, 11623 (1994).

15 T. Clark, J. Chandresekhar, and P. v. R. Schleyer, *J. Com-*

put. Chem., **4**, 294 (1983).
16 B. J. Lynch, Y. Zhao, and D. G. Truhlar, *J. Phys. Chem.*, **107**, 1384 (2003).
17 J. D. Thompson, P. Winget, and D. G. Truhlar, *Phys. Chem. Commun.*, **16**, 1 (2001).
18 J. D. Thompson, C. J. Cramer, and D. G. Truhlar, *J. Chem. Phys.*, **119**, 1661 (2003).
19 L. M. Pratt and A. Streitwieser, *J. Org. Chem.*, **68**, 2830 (2003).
20 L. M. Pratt and R. Mu, *J. Org. Chem.*, **69**, 7519 (2004).
21 I. Novak and L. M. Pratt, *Chem. Phys. Lett.*, **400**, 558 (2004).
22 L. M. Pratt and S. R. Kass, *J. Org. Chem.*, **69**, 2123 (2004).
23 J. F. Remenar, B. L. Lucht, D. Kruglyak, D. B. Collum, F. E. Romesberg, and J. H. Gilchrist, *J. Org. Chem.*, **62**, 5748 (1997).
24 J. H. Gilchrist and D. B. Collum, *J. Am. Chem. Soc.*, **114**, 794 (1992).
25 P. Renaud and M. A. Fox, *J. Am. Chem. Soc.*, **110**, 5705 (1988).
26 F. E. Romesberg, M. P. Bernstein, J. H. Gilchrist, A. T. Harrison, D. J. Fuller, and D. B. Collum, *J. Am. Chem. Soc.*, **115**, 3475 (1993).
27 F. E. Romesberg and D. B. Collum, *J. Am. Chem. Soc.*, **116**, 9187 (1994).
28 F. S. Mair, W. Clegg, and P. A. O'Neil, *J. Am. Chem. Soc.*, **115**, 3388 (1993).
29 K. W. Henderson, A. E. Dorigo, Q.-Y. Liu, P. G. Williard, P. v. R. Schleyer, and P. R. Bernstein, *J. Am. Chem. Soc.*, **118**, 1339 (1996).